Anesthesiology 2006; 105:1164–75

Pharmacologic and Functional Characterization of Malignant Hyperthermia in the R163C RyR1 Knock-in Mouse

Tianzhong Yang, M.D., Ph.D., Joyce Riehl, D.V.M., Ph.D.,† Eric Esteve, Ph.D.,‡ Klaus I. Matthaei, Ph.D.,§ Samuel Goth, Ph.D.,‖ Paul D. Allen, M.D., Ph.D.,# Isaac N. Pessah, Ph.D.,** José R. Lopez, M.D., Ph.D.††*

Background: ***Malignant hyperthermia*** **is a pharmacogenetic disorder affecting humans, dogs, pigs, and horses. In the majority of human cases and all cases in animals, malignant hyperthermia has been associated with missense mutations in the skeletal ryanodine receptor (RyR1).**

Methods: **The authors used a "knock-in" targeting vector to create mice carrying the RyR1 R163C malignant hyperthermia mutation.**

Results: **Validation of this new mouse model of human malignant hyperthermia susceptibility includes (1) proof of transcription of the R163C allele and expression of ryanodine receptor protein in R163C heterozygous and R163C homozygous animals; (2) fulminant malignant hyperthermia episodes in R163C heterozygous mice after exposure to 1.25–1.75% halothane or an ambient temperature of 42°C characterized by increased rectal temperature, respiratory rate, and inspiratory effort, with significant blood biochemical changes indicating metabolic acidosis, ending in death and hyperacute rigor mortis; (3) intraperitoneal pretreatment with dantrolene provided 100% protection from the halothane-triggered fulminant malignant hyperthermia episode; (4) significantly increased sensitivity (decreased effective concentration causing 50% of the maximal response) of R163C heterozygous and homozygous myotubes to caffeine, 4-chloro-*m*-cresol, and K^+-induced depolarization; (5) R163C heterozygous and homozygous myotubes have a significantly increased resting intracellular Ca^{2+} concentration compared with wild type; (6) R163C heterozygous sarcoplasmic reticulum membranes have a twofold higher affinity (K_d = 35.4 nM) for [^{3}H]ryanodine binding compared with wild type (K_d = 80.1 nM) and a diminished inhibitory regulation by Mg^{2+}.**

Conclusions: **Heterozygous R163C mice represent a valid model for studying the mechanisms that cause the human malignant hyperthermia syndrome.**

This article is accompanied by an Editorial View. Please see: Hogan K: In hot pursuit. ANESTHESIOLOGY 2006; 105:1077–8.

MALIGNANT hyperthermia (MH) is a pharmacogenetic disorder that is triggered by exposure of susceptible individuals to volatile anesthetics, depolarizing muscle relaxants, or stress.[1,2] Exposure to these agents results in a hypermetabolic state manifested clinically by hypercapnia, contracture of skeletal muscle, lactic acidosis, and hyperthermia. Left untreated, these episodes are nearly always fatal. MH is known to occur in humans with a prevalence of 1 in 12,000–50,000 anesthetic events.[3] It has also been identified in several domestic species, namely the pig,[4] dog,[5] and horse.[6] In all species studied to date, MH has been associated with mutations in proteins that influence excitation–contraction coupling, particularly in the skeletal isoform of the sarcoplasmic reticulum Ca^{2+} release channel, or ryanodine receptor (RyR1). Porcine,[4] canine,[5] and equine[6] MH are each thought to be caused by a missense mutation in RyR1, which can be homozygous (porcine) or heterozygous (canine and equine), whereas in humans, more than 60 RyR1 mutations and 2 α_{1s}-dihydropyridine receptor (Cav1.1) mutations have been correlated with MH susceptibility.[7,8]

Biochemical assessment of RyR1 activity in sarcoplasmic reticulum vesicles isolated from MH-susceptible (MHS) individuals has been characterized, and MHS mutations decrease in the observed EC_{50} for Ca^{2+}-dependent activation of [^{3}H]ryanodine binding.[9] In addition, MHS RyR1 ($_{MH}$RyR1) also displays attenuated inhibition by mM Ca^{2+} and Mg^{2+}, as quantified by an increase in observed IC_{50} and a failure to achieve complete inhibition in [^{3}H]ryanodine binding experiments.[9,10] Failure of $_{MH}$RyR1s to be as tightly regulated in terms of calcium gating as wild-type RyR1 ($_{WT}$RyR1) is thought to result in an ongoing trace amount of calcium release, which may in part be responsible for the increased resting Ca^{2+} concentrations observed in MHS skeletal muscle and skeletal myotubes.[11–13]

Adequate study of the mechanisms leading to the human MH syndrome requires the use of a valid animal model to study the disorder. Although the use of the naturally occurring porcine model has been historically

* Instructor, ‡ Postdoctoral Fellow, # Professor, Department of Anesthesia, Perioperative and Pain Medicine, Brigham & Women's Hospital, Boston, Massachusetts. † Project Scientist, ‖ Research Specialist, ** Professor, Department of Molecular Biosciences, School of Veterinary Medicine, University of California, Davis, California. § Associate Professor, Gene Targeting Laboratory, The John Curtin School of Medical Research, The Australian National University, Canberra, Australian Capital Territory, Australia. †† Professor, Department of Anesthesia, Perioperative and Pain Medicine, Brigham & Women's Hospital, Boston, Massachusetts. Centro de Biophysica y Bioquemica, Instituto Venezolano de Investigaciones Científicas, Caracas, Venezuela.

Received from the Department of Anesthesia, Perioperative and Pain Medicine, Brigham and Women's Hospital, Boston, Massachusetts. Submitted for publication May 31, 2006. Accepted for publication August 16, 2006. Supported by grant Nos. 1RO1AR46513 and 1P01AR52354 (to Drs. Allen and Pessah) and 1P01 ES11269 (to Dr. Pessah) from the National Institutes of Health, Bethesda, Maryland; and a fellowship grant, SPE20040901554 (to Dr. Esteve), from the Fondation Recherche Medical, Paris, France. Drs. Yang and Riehl made equal contributions to the study, and the order of authorship was determined by drawing lots.

Address correspondence to Dr. Allen: Department of Anesthesia Perioperative and Pain Medicine, Brigham & Women's Hospital, 75 Francis Street, Boston, Massachusetts 02115. allen@zeus.bwh.harvard.edu.. Individual article reprints may be purchased through the Journal Web site, www.anesthesiology.org.

useful, especially in the development of dantrolene as a therapy,[14] the use of pigs is cumbersome. Furthermore, porcine MHS is an autosomal recessive trait and limited to a single mutation, R615C, that accounts for less than 2% of human MH cases. In contrast, mouse animal models are less cumbersome and can potentially be used to study several human MH mutations due to the availability of well-established genetic manipulation techniques in the mouse. The mouse model reported in this study is one of three mice, one from each of the three "MH hot spots"[15] that we are making or have made, and it is the first to be characterized. R163C was picked because it was one of the most common MH mutations in hot spot 1,[15] and for that reason only. In this report, we characterize the clinical, biochemical, and functional properties of MHS in the R163C "knock-in" (KI) mouse.

Materials and Methods

Generation of Mice

All experiments on animals from creation of MH mice to establishment of their physiologic and biochemical phenotypes were conducted using protocols approved by the institutional animal care and use committees at the Australian National University, Harvard Medical School, and the University of California at Davis.

To generate a mouse with a KI mutation, a targeting vector carrying the mouse genomic DNA fragment harboring the mutation must be constructed and transfected into mouse embryo stem cells by electroporation (exposure of the cells to an electric shock). After entering the cell, the transfected construct DNA is transported to the nucleus and is inserted at its specific location in the mouse genome by homologous recombination. In the embryonic stem cells, the insertion of this piece of genomic DNA into its native position happens in the same way that these cells regulate their normal DNA replication and repair. It should be pointed out that homologous recombination of transfected DNA is a rare spontaneous event, and selection of few cells where it has occurred is done with positive and negative selection agents.

In this study, a 9.5-kilobase (kb) *EcoR*I fragment harboring RyR1 exons 3–13 (fig. 1A) isolated from a 129Sv/J mouse genomic library was used to construct the targeting vector. Site directed mutagenesis (QuickChange Multi Site Directed Mutagenesis Kit; Stratagene, La Jolla, CA) was used to mutate the arginine at codon 163 in exon 6 to cysteine (R163C). In total, four nucleotides were modified to generate the mutation and a new *BsmB*I restriction site (cgagttggggat to tgcgttggagac [mutations underlined]). A bacterial LoxP (locus of crossover in P1) recombination site flanked neomycin (G418) and cytosine deaminase (neo/CD) cassette was inserted at the *Eag*I site in intron 6, which is 230 base pairs (bp) downstream of the mutation site and safely away from the branch point/polypyrimidine tract needed for proper RNA splicing (fig. 1A). A thymidine kinase cassette was placed downstream from the 3′ arm in the vector backbone as a negative selection marker to help eliminate some cells that have undergone random integration events rather than homologous recombination. The vector was linearized by *Sac*II digestion, electroporated into W9.5 129Sv ES cells,[16] and subjected to positive selection with G418 and negative selection with ganciclovir using standard techniques as previously described.[17] Polymerase chain reaction (PCR) and Southern blot analysis were used to identify homologous recombination at this location. A clone identified as carrying the R163C mutation was injected into C57BL/6 murine blastocysts and implanted into pseudopregnant mice. Male chimeric mice were mated with female C57BL/6 mice, and germ line transmission was confirmed by the presence of agouti coat color, PCR screening, and Southern blot analysis. These mice were then bred to Tnap-Cre (tissue-nonspecific alkaline phosphatase promoter driven Cre recombinase) transgenic mice,[18] which had been backcrossed to the C57BL/6 background for 10 generations, to excise the LoxP-flanked neo/CD cassette. The resulting progeny with the neomycin cassette excised were then crossed two more times to the C57BL/6 background strain. Thus, the background of the R163C Het and Hom mice used in these studies was N4.C57BL/6//129Sv.

Generation of Primary Myotubes

Isolation of primary myoblast cell lines and differentiation into myotubes were performed using muscle from day 0 neonatal mice using methods described previously.[19]

RNA Isolation and Reverse-transcriptase Coupled PCR

RNA was isolated from neonatal WT, R163C heterozygous (Het), and R163C homozygous (Hom) primary myotubes using TRIzol (Invitrogen, Carlsbad, CA). Primers were purchased from Integrated DNA Technologies (Coralville, IA). Reverse-transcriptase coupled PCR reactions were performed using GeneAmp RNA PCR Kit (Applied Biosystems, Foster City, CA).

Whole Membrane Fraction Isolation and RyR1 Detection

Whole membranes were isolated from five individual R163C Het mice and five age- and strain-matched control mouse skeletal muscles isolated from E18 embryos using previously described methods.[6] RyR1 expression was detected by gel electrophoresis and Western blotting as previously described.[6] Digital scanning using EDAS software (Kodak Scientific Imaging, New Haven CT) was used to analyze Western blots from three separate mice of each genotype. The average pixel density is presented

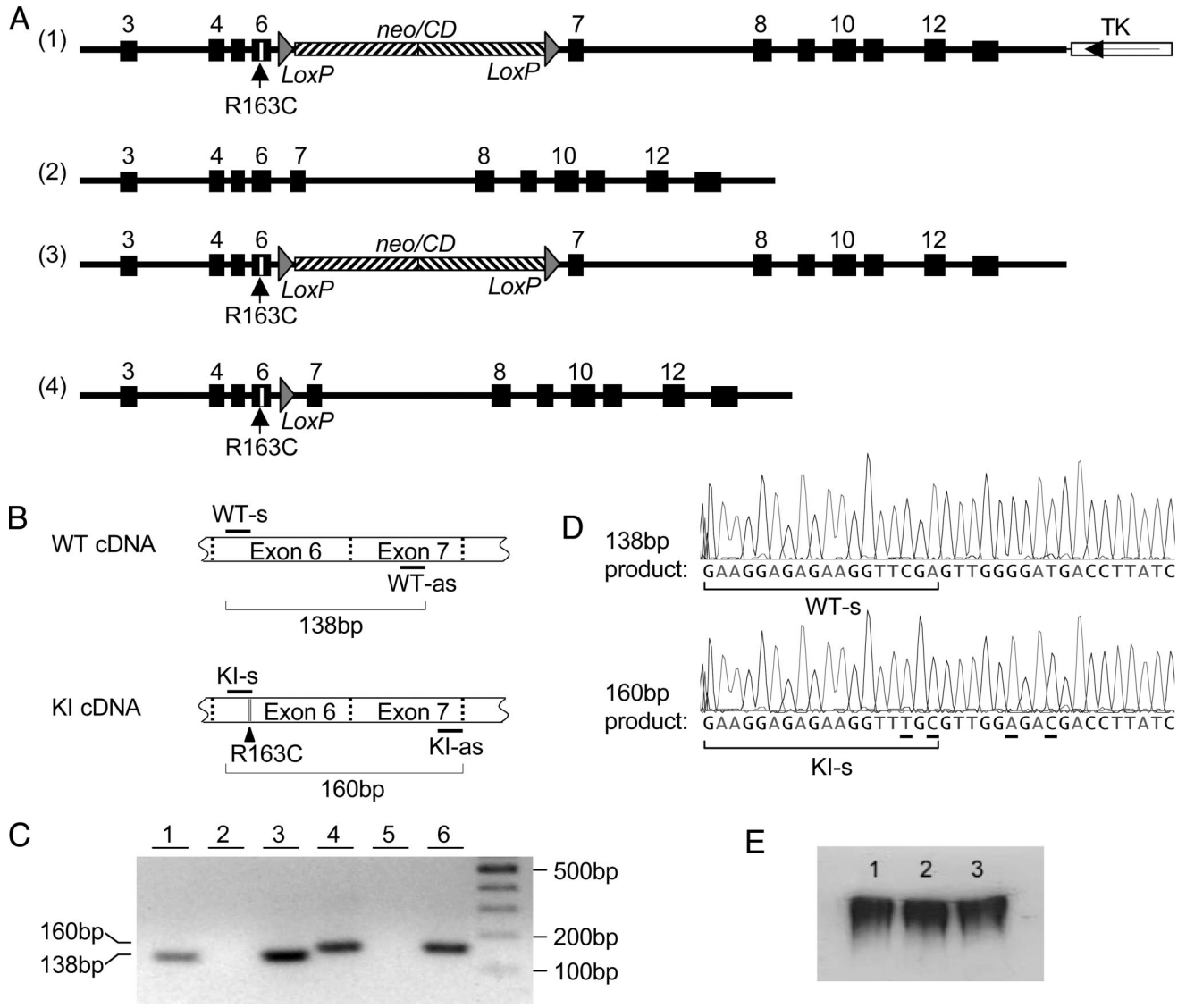

Fig. 1. Generation of R163C mice. (*A*) Construct design and recombination schematic. (*1*) Targeting construct to introduce R163C mutation into ryanodine receptor type 1 (RyR1) exon 6. (*2*) Wild-type (WT) RyR1 locus. (*3*) The same locus after recombination. (*4*) The same locus after breeding R163C mice to Tnap-Cre (tissue-nonspecific alkaline phosphatase promoter driven bacterial Cre recombinase gene) mice to remove neomycin/cytosine deaminase (*neo/CD*) cassettes. (*B*) Primer designation for reverse-transcriptase polymerase chain reaction to confirm transcription of WT and the R163C knock-in (KI) allele. (*C*) Result of reverse-transcriptase polymerase chain reaction for WT (*lanes 1* and *2*), R163C heterozygous (*lanes 3* and *4*), and R163C homozygous (*lanes 5* and *6*) mice. Primer pair WT-s/WT-as was used for *lanes 1*, *3* and *5*. Primer pair KI-s/KI-as was used for *lanes 2*, *4*, and *6*. (*D*) Partial sequencing result of all four bands from reverse-transcriptase polymerase chain reaction showing the transcribed WT and KI allele. Bands in *lanes 1* and *3* (in *B*) are identical and partially shown in the *upper panel*. Bands in *lanes 4* and *6* (in *B*) are identical and partially shown in the *lower panel*. The exact locations of primer WT-s and KI-s are labeled. The mutated four nucleotides in the 160–base pair (bp) product are *underlined*. (*E*) Western blot analysis of RyR1 expression in age-matched R163C homozygous (*lane 1*), R163C heterozygous (*lane 2*), and WT (*lane 3*) mouse embryos. Polyacrylamide gel, 7%, was used. Protein, 25 μg, was loaded in each lane. cDNA = complementary DNA; loxP = locus of crossover in P1.

as the mean ± SD of the three determinations for each group.

In Vivo *Halothane and Temperature Challenges*

Baseline blood measurements were made in WT and R163C Het animals (n = 3 per group) by collecting blood immediately after cervical dislocation by guillotine. WT and R163C Het animals (n = 6 per group) with and without pretreatment with 4 mg/kg dantrolene intraperitoneally were anesthetized using 100 mg/kg ketamine and 5 mg/kg xylazine intraperitoneally. When the animals were immobilized, they were placed on a circulating water bath, covered with a blanket, and instrumented with a thermistor to constantly monitor rectal temperature. Blood (120 μl) was collected from the orbital sinus for the before halothane measurements. Halothane, 2% in oxygen, was delivered by facemask *via* a precision vaporizer at a rate of 1.5 l/min for 2 min. At this time, the halothane concentration was reduced to between 1.25% and 1.75% as needed to abolish a toe

pinch response. Halothane exposure was continued for 20 min or until the animals exhibited signs of a fulminant MH episode (defined as tachypnea [measured in breaths/min], hyperthermia, and muscle rigidity). Rectal temperature was monitored by thermistor, rigidity was monitored by manually testing limb resistance, and respiratory rate and character were monitored visually during anesthesia. When the R163C Het animals began to show signs of fulminant MH (11.3 ± 2.6 min; mean ± SD) or in WT immediately before euthanasia after discontinuation of halothane exposure, blood (200 μl) was collected *via* cardiac puncture. Blood gas analyses were performed on blood samples using a Radiometer ABL 700 blood gas analyzer (Diamond Diagnostics, Holliston, MA).

Differences in the responses of WT and R163C Het mice exposed to increased temperature were determined by transferring individual test animals (n = 6 of each genotype) from their cages at 24°C into a test chamber equilibrated at 42°C. Animals were kept at the increased temperature for a maximum of 15 min (for WT) or until a fulminant MH episode was triggered. Rectal temperatures were measured by thermistor before and upon removal from the chamber and are presented as mean ± SD.

Calcium Imaging of Myotubes

Stock concentrations of caffeine and 4-chloro-*m*-cresol (4-C*m*C) solutions were prepared in imaging buffer (125 mM NaCl, 5 mM KCl, 2 mM $CaCl_2$, 1.2 mM $MgSO_4$, 6 mM glucose, and 25 mM HEPES, pH 7.4). In KCl-containing solutions, the concentration of NaCl was adjusted as necessary to maintain a total ionic strength ($K^+ + Na^+$) at 130 mM.

Differentiated myotubes were loaded with 5 μM Fluo-4 AM (Molecular Probes Inc., Eugene, OR) at 37°C, for 20 min in imaging buffer. The cells were then washed three times with imaging buffer and transferred to a fluorescence microscope, and Fluo-4 was excited at 494 nm using a Multivalve Perfusion System (Automate Scientific Inc., Oakland, CA). Fluorescence emission was measured at 516 nm using a 40× 1.3na oil objective. Data were collected with an intensified 12-bit digital intensified charge-coupled device (Stanford Photonics, Stanford, CA) from regions consisting of 10–20 individual cells, and analyzed using QED software (QED, Pittsburgh, PA). A dose–response curve for a single agent was performed in every well to compare the response to any given agent to primary myotubes expressing $_{WT}$RyR1, heterozygous R163C RyR1, or homozygous R163C RyR1 protein. The average fluorescence of the calcium transient (defined by the area under the transient curve) was compared among genotypes. Individual areas under the curve were calculated in the following way: the average fluorescence during the 10-s challenge minus the average baseline fluorescence for the 1 s immediately before the challenge. Because of variability in responses from cell to cell, to compare different experiments, individual response amplitudes were normalized to the maximum response amplitude obtained in that cell at the highest concentration of the reagent that was being tested (15 mM caffeine, 500 μM 4-C*m*C, and 80 mM KCl). All data were obtained from differentiated myotubes in 5–10 different wells (in 96-well plates). Data are presented as mean ± SD.

[^{3}H]Ryanodine Binding

Using pooled whole membrane fractions from five R163C Het mice, we assessed the sensitivity of RyR1 activity to modulation by effectors such as Mg^{2+}, and 4-C*m*C using [^{3}H]ryanodine binding. The optimal protein concentration for binding experiments was determined by incubating aliquots of 50–200 μg/ml whole-membrane fractions at 37°C for 3 h with constant shaking in buffer consisting of 1 M KCl, 20 mM HEPES, 50 μM Ca^{2+}, and 2.5 nM [^{3}H]ryanodine (PerkinElmer Life and Analytical Sciences, Inc., Wellesley, MA). Nonspecific ryanodine binding was quantified using 1,000-fold excess unlabeled ryanodine. Bound and free ligand were separated by rapid filtration through Whatman GF/B glass fiber filters using a Brandel cell harvester (Whatman, Gaithersburg, MD) and rapidly washed with 3 × 5 ml ice-cold buffer (20 mM HEPES, 140 mM KCl, 15 mM NaCl, and 50 μM Ca^{2+}, pH 7.4). Radioactivity was quantified by liquid scintillation spectrometry using a scintillation counter. Data were analyzed and curve fitted using the computer program Origin 7.0 (Origin Lab Corp., Northampton, MA).

Equilibrium [^{3}H]ryanodine binding was performed as above by incubating membrane preparations (180 μg/ml) with 1 nM [^{3}H]ryanodine (PerkinElmer Life and Analytical Sciences, Inc.) in the presence of 0–99 nM unlabeled ryanodine in a binding buffer containing 250 mM KCl, 50 μM Ca^{2+}, and 20 mM HEPES, pH 7.4. Modulation of ryanodine binding to RyR1 by Ca^{2+}, Mg^{2+}, and 4-C*m*C was analyzed in the above binding buffer containing free Ca^{2+} and Mg^{2+} concentrations based on calculations from "bound and determined" software.[20]

Histopathology and Fiber Type Analysis

Muscles from two WT and two R163C Het mice were frozen and imbedded. Serial sections were cut and then stained with hematoxylin and eosin, modified trichrome stain, periodic acid–Schiff reagent, phosphorylase, adenosine triphosphatase at pH 9.8, 4.6, and 4.3, esterase, reduced nicotinamide adenine dinucleotide, alkaline phosphatase, acid phosphatase, oil red-O, and succinic dehydrogenase.

Ca^{2+}-selective Microelectrodes and Intracellular Free Ca^{2+} Measurements

Double-barreled Ca^{2+}-selective microelectrodes were prepared and selected as described previously.[13] Myo-

tube impalements were observed through an inverted microscope fitted with a 10× eyepiece and a 40× dry objective. The potentials from the 3 M KCl barrel (V_m) and the Ca^{2+} barrel (V_{Cae}) were recorded *via* a high-impedance amplifier ($> 10^{11}$ MΩ, model FD-223; WPI, Sarasota, FL). The potential of the voltage microelectrode (V_m) was subtracted electronically from the potential of the Ca^{2+} electrode (V_{Cae}) to give the differential signal (V_{Ca}) that represents the resting myoplasmic Ca^{2+} concentration. V_m and V_{Ca} potentials were filtered using a low-pass filter (LPF-30-WPI) at 10–30 KHz, acquired with a frequency of 1,000 Hz with AxoGraph (version 4.8; Axon Instruments, Foster City, CA), and stored for further analysis.

Statistical Analysis

The Student *t* test was used to compare the temperature and blood gas results between WT and R163C Het. Prism software (version 4.0b; GraphPad Software, San Diego, CA) was used for nonlinear regression with sigmoidal dose–response analysis of imaging results. One-way analysis of variance and Tukey multiple comparison tests were used to compare the Log(EC_{50}) and resting intracellular Ca^{2+} concentration ($[Ca^{2+}]_i$) among cells with different genotypes. The amount of bound ryanodine was determined and curve fitted using the computer program Origin 7.0, and the Student *t* test was used for statistical analyses.

Results

Confirmation of Transcription of the R163C Knock-in Allele and Expression of RyR1 Protein

To confirm the transcription, and presumably the expression of the R163C KI allele in R163C Het and R163C Hom mice, reverse-transcriptase coupled PCR was performed using the extracted messenger RNA from differentiated WT, R163C Het, and R163C Hom primary myotubes (fig. 1). As shown in figure 1B, primers were designed across the exon 6/7 boundary, to help differentiate PCR products from complementary DNA (cDNA) and those from possible contaminating genomic DNA, as the latter product (including intron 6) should be longer by 350 bp. The two upper primers for WT and KI cDNAs, WT-s and KI-s, terminate at the R163C mutation (figs. 1B and C) to facilitate the detection of the genotype, because each primer works only with the corresponding allele. The two lower primers, WT-as and KI-as, were designed at different locations in exon 7, to facilitate distinguishing between WT and KI PCR products by size (138 and 160 bp, respectively). As shown in figure 1D, only the 138-bp WT band was produced from myotubes of WT mice (lanes 1 and 2), only the 160-bp KI band was amplified from myotubes of R163C Hom mice (lanes 5 and 6), and both bands were yielded from myotubes of R163C Het mice (lanes 3 and 4). Sequencing of all four fragments confirmed the correct exon 6–7 region for both WT and KI alleles and is shown in figure 1D.

There is no overt pathologic phenotype observed in heterozygous R163C mice under typical rearing conditions. R163C Hom mice that were detected by PCR (not shown) had an embryonic-lethal phenotype and likely die *in utero* at approximately days E17–18. Although R163C has also been associated with central core disease (CCD) in humans,[15] examination of muscles from both R163C Het and Hom mice did not show any detectable core formation, similar to what was previously reported in Y522S MH/CCD mice.[21] There were also no differences in fiber type, nor any other analysis done by histopathology between R163C and WT. Western blot analysis performed with muscle membranes isolated from R163C Hom, R163C Het, and age-matched WT mouse embryos (fig. 1E) showed no differences in the level of expression of RyR1 protein (densitometry analysis: R163 Hom 116.9 ± 14.3 *vs.* R163C Het 125.8 ± 12.7 *vs.* WT 118.7 ± 10.2 pixels).

Clinical MH in R163C Het Mice Exposed to Halothane Challenge and Increased Temperature

Although the clinical presentation of the MH syndrome varies with genetic and environmental variables, the most common manifestations include tachycardia, increased respiratory rate, increased body temperature, and skeletal muscle rigidity.[7] Recently, Chelu *et al.* [21] reported evidence of malignant hyperthermia in RyR1 Y522S heterozygous mice after exposure to clinical levels of isoflurane. Although the study did not present a detailed clinical account of the fulminant episode, Y522S mice exhibited hyperacute rigor mortis and increased rectal temperature as an end result of the anesthetic. In the current study, we extend the clinical characterization of MH in the mouse. We used a precision vaporizer to deliver 2% halothane in oxygen followed by maintenance with 1.25–1.75% halothane and monitored rectal temperature, respiratory rate, and venous blood gases to obtain detailed clinical characteristics of murine MH in the R163C Het mice.

All WT animals had uneventful anesthetic courses. We observed a slight increase in the respiratory rate in the WT animals during the orbital sinus blood collection, but all WT animals tolerated the blood collection well. At the end of the 20-min halothane exposure, a cardiac puncture was performed and the WT animals were killed. WT animals maintained respiratory rates at 152 ± 21 (mean ± SD) breaths/min. In contrast, all R163C Het animals displayed clinical signs that were consistent with a fulminant MH episode. R163C Het animals displayed an increase in respiratory rate from 147 ± 23 to 183 ± 23 breaths/min. Three of the six animals died during or immediately after the orbital sinus blood collection. The

other three animals died from their fulminant MH episode during what should have been the recovery period (range, 6.8–19.4 min after discontinuation of halothane). All six MH animals exhibited increased respiratory rate and inspiratory effort. Five of the six animals exhibited hyperacute rigor mortis, with full body contracture within 0.34 min of the last breath (range, −4 to 3.05 min) (fig. 2A). Animal 3 underwent a 20-min halothane exposure and recovered from anesthesia. The anesthetic recovery was slow, and the animal seemed to be less active than a matched control animal at 5 h after the anesthetic event. This decrease in activity may be due to rhabdomyolysis, which is known to be a component of the fulminant MH episode.[22] This animal was rechallenged 24 h later, and again underwent another full 20-min exposure to halothane. The animal died after exhibiting an increase in rectal temperature and respiratory rate and effort 7.1 min after halothane was discontinued.

Wild-type animals maintained rectal temperatures ranging from 32° to 37°C (fig. 2B) during general anesthesia. R163C Het animals began halothane exposure with temperatures ranging from 33° to 36°C. All six R163C Het animals showed a significant increase in rectal temperature after halothane exposure (fig. 2B), whereas temperatures in WT animals decreased slightly. Mean peak rectal temperature after halothane exposure was 35.0° ± 1.8°C for WT and 37.8° ± 0.8°C for R163C Het (mean ± SD; n = 6 per group; $P = 0.0024$ by Student t test). In all anesthetics that resulted in a fulminant MH episode, the peak rectal temperature was followed within 4.4 ± 2.4 min (range, 0.8–17.6 min) by a decline in rectal temperature of 0.48° ± 0.13°C and respiratory arrest.

Blood gas analysis was performed in all animals during the halothane exposure and immediately before euthanasia. The results of the blood gas analysis are displayed in table 1. WT and R163C Het mice showed mild acidemia at baseline, whereas blood gases from cohorts of mice killed by cervical dislocation showed pH of 7.33 ± 0.55 in R163C Het mice *versus* 7.38 ± 0.07 in WT animals ($P = 0.62$). The WT animals showed no significant change from control values in blood pH or blood partial pressure of carbon dioxide during the anesthetic period (pH = 7.25 ± 0.03 before halothane *vs.* 7.32 ± 0.17 immediately before euthanasia; $P = 0.35$; blood partial pressure of carbon dioxide = 35.4 ± 4.1 mmHg *vs.* 43.3 ± 14.7 mmHg, $P = 0.30$). However, the R163C Het mice displayed a significant change in blood pH and blood partial pressure of carbon dioxide (table 1). The R163C Het animals differed significantly from WT in their blood pH, blood partial pressure of carbon dioxide, blood lactate, and blood HCO_3 immediately before death, with values demonstrating both metabolic and respiratory acidosis (table 1).

The skeletal muscle relaxant dantrolene is known to help prevent or reverse the clinical signs associated

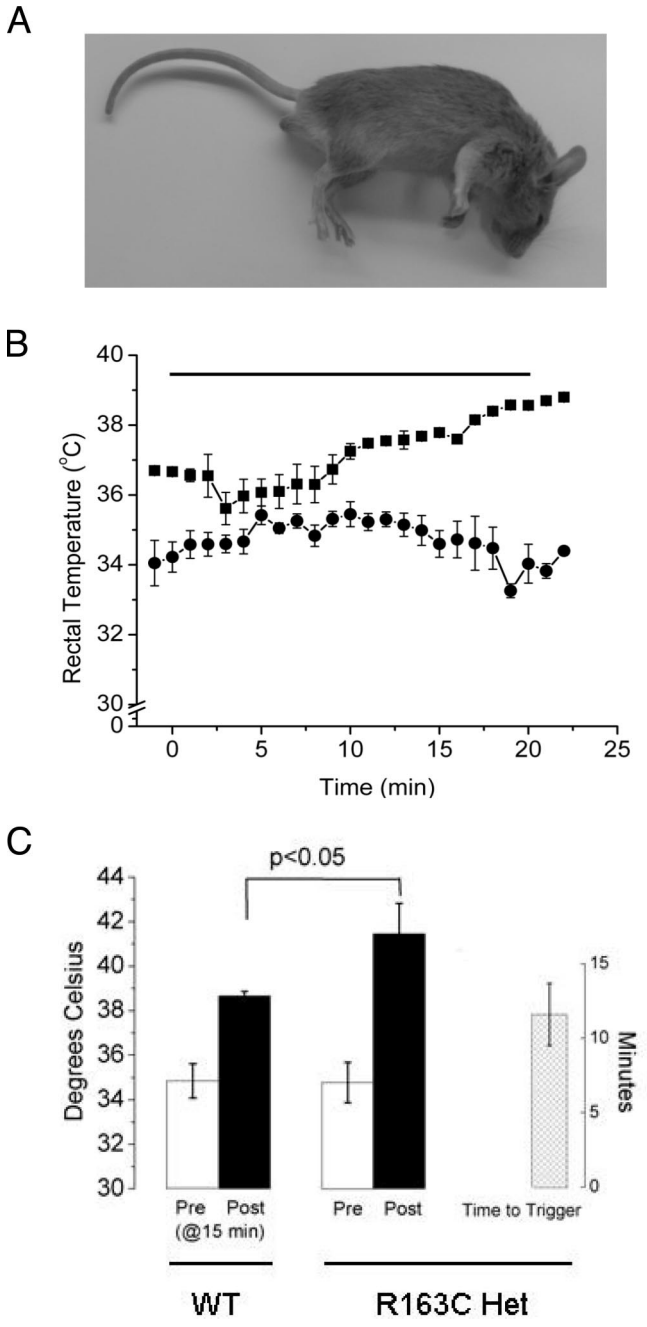

Fig. 2. *In vivo* halothane challenge of wild-type (WT) and R163C heterozygous (Het) mice. (*A*) Hyperacute rigor mortis of a representative R163C Het mouse evidenced by contracture of skeletal muscles, notably the face, neck, and limbs. (*B*) Rectal temperature of R163C Het (■) and control (●) mice after exposure to halothane. Data are pooled into 1-min bins and displayed with SDs. The period of exposure to halothane is denoted by the *bar* above. (*C*) Rectal temperatures of WT and R163C Het mice before (*white bars*) and immediately after terminating the exposure to 42°C (*black bars*).

with MH.[25] To determine whether dantrolene results in protection from a fulminant MH episode, animals (n = 6) were pretreated with 4 mg/kg intraperitoneal dantrolene given 30 min before premedication with ketamine and xylazine. The halothane exposure was then performed according to the above protocol. Dan-

Table 1. Venous Blood Gas Analysis and Respiratory Rates

	Baseline			Before			After		
	R163C Het	WT	*P*	R163C Het	WT	*P*	R163C Het	WT	*P*
pH	7.33 ± 0.5	7.38 ± 0.1	0.62	7.18 ± 0.03	7.25 ± 0.03	0.12	6.92 ± 0.1	7.32 ± 0.2	< 0.01
P_{CO_2}, mmHg	37.3 ± 3.2	36.0 ± 2.8	0.59	47.6 ± 3.8	35.4 ± 4.1	0.06	131.57 ± 61.8	43.3 ± 14.7	0.01
Lactate, mM	3.0 ± 0.5	3.5 ± 1.4	0.51	4.8 ± 1.5	3.4 ± 0.4	0.32	6.4 ± 2.9	0.7 ± 0.2	< 0.01
BE, mM	−6.6 ± 2.0	−7.6 ± 0.8	0.24	−10.0 ± 1.5	−10.6 ± 2.3	0.84	−7.9 ± 7.7	−2.9 ± 10.02	0.38
HCO_3, mM	18.1 ± 1.8	14.0 ± 5.3	0.27	14.9 ± 1.0	15.6 ± 1.8	0.77	12.8 ± 4.4	21.9 ± 8.4	0.05
RR, breaths/min	134 ± 28	142 ± 13	0.36	149 ± 22	136 ± 26	< 0.01	184 ± 22	147 ± 21	< 0.01

Results of venous blood gases test for wild type and R163C heterozygous (Het) mice (n = 3) after death by decapitation with no anesthesia (Baseline), and from a second group of mice (n = 6) after premedication with ketamine–xylazine but before halothane (Before) and after halothane exposure (After). Data are presented as mean ± SD.

BE = base excess; P_{CO_2}= partial pressure of carbon dioxide; RR = respiratory rate; WT = wild type.

trolene administration resulted in no significant gross differences in observed gait and activity level when compared with the animals that were not pretreated. None of the R163C Het animals that were pretreated with dantrolene exhibited clinical signs consistent with MH before or after the halothane challenge. Rechallenge of the same animals 24 h later without dantrolene pretreatment resulted in the development of hyperthermia, increased respiratory rate, and hyperacute rigor mortis in 100% of the animals.

The R163C Het mice also responded with what seemed to be a fulminant MH syndrome with a short exposure to an ambient temperature of 42°C. None of the WT mice we tested exhibited any adverse responses when exposed to 42°C for 15 min, although their rectal temperatures did increase by 3.4°C ($P \leq 0.05$; fig. 2C). By contrast, all R163C Het mice (n = 4) challenged by an increased ambient temperature exhibited an abrupt development of an increase in both their spontaneous activity and observed respiratory rate ending in hyperacute rigor mortis with a mean latency of 11.5 ± 1.8 min after commencement of the exposure. The core temperature of R163C Het mice at the time of death was significantly increased compared with their initial temperature measured under ambient conditions (+7.5°C; $P \leq 0.05$; fig. 2C), and this increase was significantly greater than the small increase seen in WT mice ($P < 0.01$).

Myotubes from R163C Mice Show Heightened Sensitivity to RyR1 Activators

One of the most common functional abnormalities associated with MH mutations is the increased sensitivity in Ca^{2+} response of muscle cells to stimulation with caffeine, 4-C*m*C, and K^+-induced depolarization.[10] To further characterize the functional features of the muscle cells of R163C KI mice, Ca^{2+} imaging experiments were performed using differentiated myotubes from primary myoblasts generated from neonatal WT, R163C Het, and R163C Hom neonatal mice. No observed difference in the cell shape and size was found between these three types of primary myoblasts or myotubes. As shown in figure 3A, significant Ca^{2+} transients (responses greater than 5% of base fluorescence value) to caffeine were observed in response to 5 mM caffeine in WT myotubes, whereas the corresponding caffeine concentrations for R163C Het and R163C Hom are 2 and 1 mM, respectively. This suggests that the threshold of Ca^{2+} response to caffeine is decreased in R163C Het myotubes and further decreased in R163C Hom myotubes. The thresholds for different genotypes are so different (5, 2, and 1 mM for WT, R163C Het, and R163C Hom, respectively) that the caffeine concentration range for R163C Het and R163C Hom myotubes had to be reduced to 0.5–8.0 mM from the 2.0–15.0 mM concentrations used for WT myotubes. Comparison of Log(EC_{50}) values using one-way analysis of variance revealed a significantly decreased EC_{50} ($P < 0.001$) for R163C Het compared with WT (3.3 *vs.* 6.5 mM) and even further decreased EC_{50} ($P < 0.001$) for R163C Hom compared with R163C Het (2.5 *vs.* 3.3 mM). A similarly significant difference in threshold and EC_{50} was found for 4-C*m*C–stimulated Ca^{2+} responses between WT, R163C Het, and R163C Hom myotubes (thresholds at 100, 50, and 5 μM, respectively; EC_{50}s at 240.6, 135.8, and 27.0 μM, respectively), as shown in figure 3B. Interestingly, the Hill coefficients of 4-C*m*C dose–response curves differed significantly among the three myotube genotypes (n_H = 6.11, 2.85, and 1.60 for WT, R163C Het, and R163C Hom, respectively). By comparison, the difference among Hill coefficients is much narrower for caffeine dose–response curves (n_H = 4.06, 4.41, and 4.82 for WT, R163C Het, and R163C Hom, respectively).

When the sensitivities of R163C Hom, R163C Het, and WT myotubes to K^+-induced depolarization were investigated, a nearly equal reduction in sensitivity among the three genotypes was found. As shown in figure 3C, both the threshold and EC_{50}s of the KCl dose–response curves are significantly decreased ($P <$ 0.001) for R163C Het and R163C Hom myotubes compared with WT ones, and significant decrease ($P <$

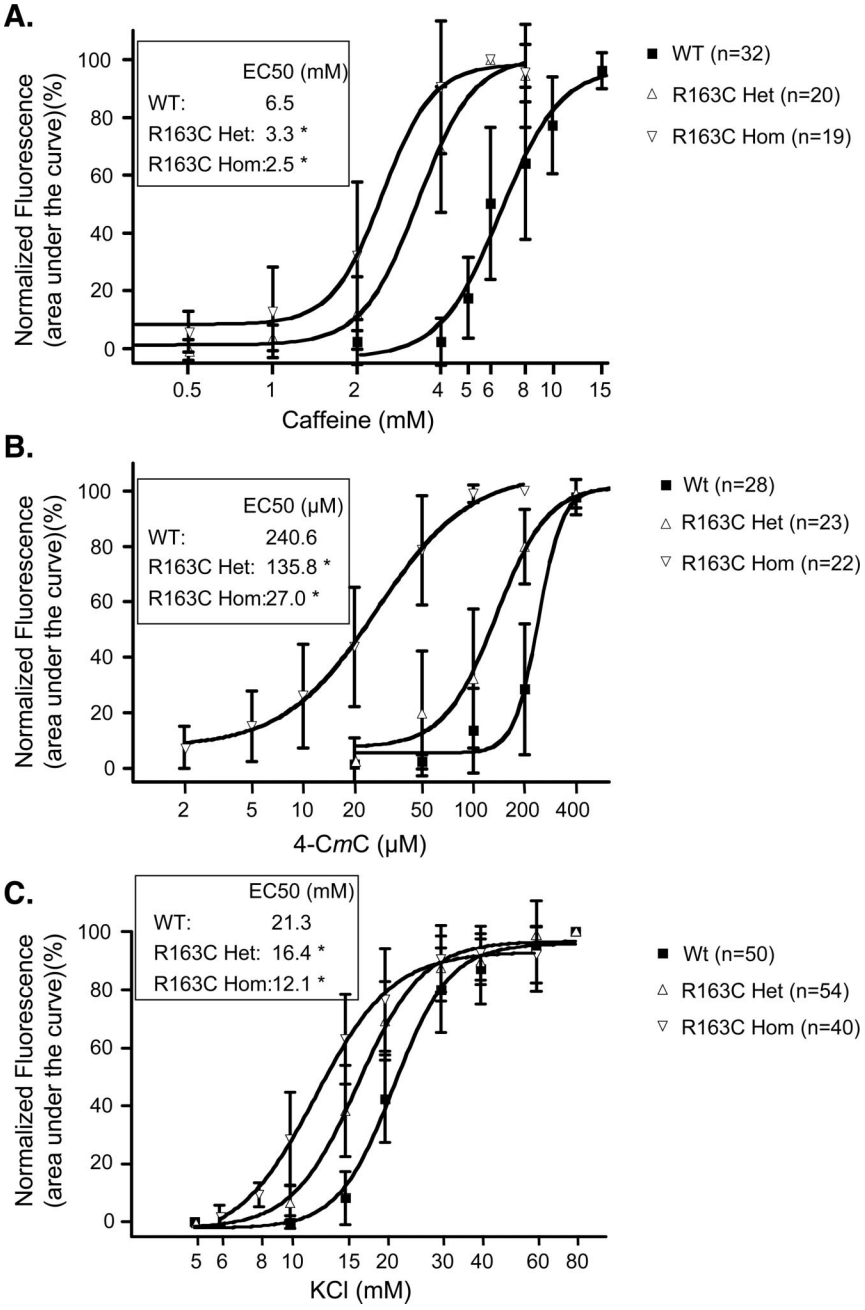

Fig. 3. Sigmoidal dose–response analysis of Ca^{2+} imaging in generated myotubes from wild-type (WT), R163C heterozygous (Het), and R163C homozygous (Hom) mice in response to caffeine (*A*), 4-chloro-*m*-cresol (4-C*m*C) (*B*), and KCl (*C*). EC_{50}s are shown in *insets*. * EC_{50} significantly different from the other two values in the same inset ($P < 0.001$, Tukey multiple comparison test of Log(EC_{50})s). Data are presented as mean ± SD.

0.001) is further observed for R163C Hom compared with R163C Het (thresholds at 15, 10, and 8 mM respectively, and EC_{50}s at 21.3, 16.4, and 12.1 mM, respectively, for WT, R163C Het, and R163C Hom).

Resting Intracellular Ca^{2+} Concentrations Are Increased in R163C Primary Myotubes

In the current study, we used double-barreled Ca^{2+}-selective microelectrodes to measure resting $[Ca^{2+}]_i$ in primary myotubes generated from neonatal WT, R163C Het, and R163C Hom mice. The resting $[Ca^{2+}]_i$ in R163C Het and Hom myotubes is significantly higher than that in WT myotubes ($P < 0.001$), and the resting $[Ca^{2+}]_i$ in R163C Hom myotubes is significantly higher than that in R163C Het myotubes ($P < 0.001$) (122.9 ± 1.8 nM [n = 10], 272.1 ± 9.2 nM [n = 10], and 335.1 ± 6.34 nM [n = 10] for WT, R163C Het, and R163C Hom, respectively [mean ± SD]).

[^{3}H]Ryanodine Binding

In this study, incubation of microsomes from WT and R163C Het with increasing concentrations of 4-C*m*C in the presence of 100 nM Ca^{2+} resulted in a dose-depen-

Table 2. [^{3}H]Ryanodine Binding Test

	R163C Het	WT	*P*
EC_{50} for 4-C*m*C activation	933.78 ± 28.81 μM	1279.22 ± 104.67 μM	0.09
IC_{50} for Mg^{2+} inhibition	0.08 ± 0.01 mM	0.05 ± 0.01 mM	0.02
Ryanodine binding affinity ($1/K_d$)	35.4 ± 0.72 nM	80.1 ± 16.3 nM	< 0.01
Maximal ryanodine binding (B_{max})	3.2 ± 0.76 pmol/mg	6.8 ± 0.40 pmol/mg	0.04

Results of [^{3}H]ryanodine binding for wild-type (WT) and R163C heterozygous (Het) vesicles. Data are presented as mean ± SD.
4-C*m*C = 4-chloro-*m*-cresol.

dent increase in [^{3}H]ryanodine binding (table 2). Whereas there was a trend toward increased sensitivity to 4-C*m*C in R163C Het membranes compared with WT, there was no significant difference between the two groups (EC_{50} = 933.8 ± 28.8 μM for R163C Het *vs.* 1279.2 ± 104.7 μM for WT; P = 0.09). In addition, incubation of RyR1 from WT and R163C Het with increasing concentrations of Mg^{2+} showed attenuation of Mg^{2+} inhibition in R163C Het membranes relative to WT (0.08 ± 0.01 mM for R163C Het *vs.* 0.05 ± 0.01 mM for WT; p = 0.02; table 2).

RyR1 from R163C Het showed a 2.3-fold increase in binding affinity relative to WT ($1/K_d$ = 35.4 nM *vs.* WT $1/K_d$ = 80.1 nM). R163C Het showed a 2.1-fold decrease in binding capacity for ryanodine relative to WT (R163C Het B_{max} = 3.2 pmol/mg protein *vs.* WT B_{max} = 6.8 pmol/mg protein) (table 2).

Discussion

Our first task was to make certain that any phenotypic differences we found in R163C KI mice were due to the expression of the mutated protein and not due to differences in the overall expression of RyR1. This was confirmed with our biochemical studies, which showed that as expected, mice that had a R163C KI allele transcribed the mutated protein, and that total amount of RyR1 protein expression was similar to that of WT animals. We also demonstrated that to the degree that it was tested, R163C Het mice, like MHS humans, do not seem to have any differences in birth rate or life expectancy.

Our next task was to define the physiologic responses of R163C Het animals. In this regard, before halothane exposure, R163C Het animals had rectal temperatures that were on average 2°C higher than the rectal temperatures measured in the WT animals at the same time point. This could suggest that there was a difference in the metabolic rate in the R163C Het mice. We believe that this is not the case and that the slightly higher mean temperatures in the xylazine-ketamine–sedated MH mice just before halothane administration, although statistically significant, do not have any real "clinical" significance both because our studies on awake animals showed no differences in temperature without sedation and because the temperature had reached a plateau and even began to decrease after the initial exposure to halothane. Although it is theoretically possible that the higher temperatures in R163C Het mice were the result of the animals having triggered the MH syndrome in response to the stress associated with the administration of ketamine–xylazine and then recovering spontaneously before the halothane challenge, we believe this to be unlikely. It is more likely that this was a systematic difference based on when the animals were tested and the duration between their placement on the warming pad and placement of the rectal probe.

After halothane exposure, all R163C Het animals showed a significant increase in rectal temperature, whereas the rectal temperatures of WT animals decreased slightly. This temperature trend is in accordance with that reported in the WT and Y522S Het MH mice exposed to isoflurane[21] at the time when the latter group displayed hyperacute rigor mortis. In both the Y522S Het mouse and our R163C MH mouse studies, the peak rectal temperatures are lower than what has been reported during an MH crisis in other species.[6,23] Rectal temperature reflects a balance between heat generation and loss. The higher surface area–to–volume ratio in the mouse compared with other species causes increased radiative heat loss in this species. We believe that this, in combination with the vasodilatory effects of halothane, likely resulted in greater increased heat loss leading to an overall decreased measured rectal temperature than would be possible if the area-to-volume ratios where similar to those in other species.

In measuring the prehalothane blood pH levels, an unexpected finding was that both WT and R163C Het mice showed a significant acidemia at baseline. This acidosis deteriorated further after halothane exposure in the R163C Het mice, whereas it recovered to normal levels after halothane exposure in WT mice. We attribute the initial acidemia seen in both groups to the ketamine–xylazine anesthesia used to "sedate" the mice, because a similar acidemia has been reported recently by others after administration of this anesthetic pair in mice and rats.[24]

It is interesting to note that similar to the previous report by Chelu *et al.*[21] on Y522S Het MH mice, R163C Het mice were intolerant to a simple 15-min heat exposure to an ambient temperature of 42°C, which triggered an MH syndrome and sudden death without exposure to volatile anesthetics. It has long been suggested that MHS

humans are also heat intolerant, but evidence for this has been largely anecdotal rather than being based on scientific information.

In addition to showing that halothane and heat could trigger an MH syndrome in R163C mice, we also confirmed that similar to other MH susceptible animals and humans, administration of a therapeutic dose of the skeletal muscle relaxant dantrolene, which is known to help prevent or reverse the clinical signs associated with MH,[25] prevented the development of clinical signs consistent with MH in R163 Het mice after a halothane challenge. We believe that the fact that dantrolene was protective in the R163C Het mice provides further evidence that these mice are susceptible to MH and helps to validate these mice as a model system for study of MH mechanisms.

Similar to our studies with recombinant MH R163C in null myotubes[10] (which would mimic R163C Hom myotubes) and studies from other groups on other $_{MH}$RyR mutations,[26–28] the threshold of Ca^{2+} response to caffeine is decreased in R163C Het myotubes and further decreased in R163C Hom myotubes. The thresholds for the different genotypes were so different (5, 2, 1 mM for WT, R163C Het, and R163C Hom, respectively) that the caffeine concentration range studied for R163C Het and R163C Hom myotubes had to be reduced to 0.5–8.0 mM from the 2.0–15.0 mM concentrations used for WT myotubes. Likewise, there was a similarly significant difference in threshold and EC_{50} for 4-C*m*C–stimulated Ca^{2+} responses between WT, R163C Het, and R163C Hom myotubes and an increased sensitivity in their threshold for K^+ depolarization. Interestingly, the Hill coefficients of 4-C*m*C dose–response curves differed significantly among myotubes of each of the three genotypes (n_H = 6.11, 2.85, and 1.60 for WT, R163C Het, and R163C Hom, respectively). By comparison, the difference among Hill coefficients among the genotypes is much narrower for the caffeine dose–response curves (n_H = 4.06, 4.41, and 4.82 for WT, R163C Het, and R163C Hom, respectively). These data suggest that whereas both agents activate the channel, the mechanisms by which they affect RyR1 modulation are different.

Our results clearly showed for the first time that R163C Hom primary myotubes are significantly more sensitive than R163C Het myotubes to all three types of stimulation. This increased sensitivity to direct RyR1 activators is consistent with two studies on human muscle biopsies carrying heterozygous and homozygous C35R[29] and R614C[30] $_{MH}$RyR mutations. Interestingly, the thresholds of caffeine responses for WT, R163C Het, and R163C Hom myotubes observed in this study are similar to the caffeine thresholds in the *in vitro* caffeine stimulation tests performed in these two studies. (The caffeine thresholds of *in vitro* caffeine stimulation tests for WT, heterozygous, and homozygous MH [C35R[29] or R614C[30]] muscle specimens are greater than 4, 1.5–2.0, and 0.5 mM respectively, compared with 5, 2, and 1 mM observed in this study.) In contrast to our findings, a recent study by Chelu *et al.* [21] found no increased sensitivity to 4-C*m*C (500 μM) in Y522S heterozygous myotubes but showed enhanced sensitivity of the maximal sarcoplasmic reticulum Ca^{2+} release in response to caffeine and voltage. Furthermore, in contrast to both the current study and other studies on heterozygous and homozygous C35R[29] and R614C[30] human MH mutations, homozygous Y522S myotubes did not show any increased caffeine or voltage sensitivity compared with WT. This difference was attributed by the authors to be the result of decreased stores in the Y522S Hom myotubes based on their significantly decreased maximal sarcoplasmic reticulum Ca^{2+} release compared with WT in response to both electrical stimulations and maximally activating caffeine concentrations.

It has previously been shown that intracellular Ca^{2+} measurements using Ca^{2+}-selective microelectrodes and in some cases with fluorescent indicators that resting $[Ca^{2+}]_i$ is elevated in adult MH human muscle fibers[31,32] possessing unidentified mutations, in adult MH muscle fibers of MH swine (RyR1 R614C),[33] and in cultured RyR1 null cells expressing recombinant RyR1 from cDNAs encoding seven MH mutations.[34–36] The increased resting $[Ca^{2+}]_i$ in MH muscle cells has been directly associated with their increased sensitivity to caffeine/4-C*m*C stimulation.[11,13] Our results in the current study showing an elevated resting $[Ca^{2+}]_i$ in R163C primary myotubes, together with the decreased EC_{50}s for caffeine/4-C*m*C–stimulated Ca^{2+} responses in the same primary myotubes, supports both the increased $[Ca^{2+}]_i$ in muscles expressing $_{MH}$RyR1s and the previously observed association between increased sensitivity to RyR1 activators and chronically elevated resting $[Ca^{2+}]_i$ in MH muscle cells.[11–13] It also supports the hypothesis that ryanodine receptor channels with MH mutations are more "leaky" than WT channels. Furthermore, homozygous RyR1 channels are even more "leaky" than heterozygous ones.

By contrast, using the Ca^{2+}-sensitive fluorescence dye indo-1 to estimate $[Ca^{2+}]_i$ in Y522S heterozygous and homozygous myotubes, resting $[Ca^{2+}]_i$ was not significantly increased compared with WT myotubes.[21] This difference from the current study may either reflect the difference in the method used for measurement of $[Ca^{2+}]_i$ or further support divergent phenotypes between these two MH mutations.

The plant alkaloid ryanodine specifically binds RyR with high affinity when it is in an open (active) conformation.[37] [^{3}H]Ryanodine binding is therefore a quantitative index of RyR1 activity *in vitro*. RyR1 from MHS individuals is known to have increased sensitivity to activation and decreased sensitivity to inhibition by known modulators of RyR1 activity such as 4-C*m*C and Mg^{2+}.[10,38]

These results are in accordance with previously published data indicating RyR1 from MHS shows increased propensity to activation and a decreased propensity to inactivation.[10,38] In addition, several reports have also shown that RyR1 from MHS individuals shows a twofold to fourfold increase in ryanodine affinity when compared with controls.[6,39] In accordance with previous reports, we found that the affinity of equilibrium binding of [^{3}H]ryanodine of RyR1 from R163C Het mice showed a 2.3-fold increase in binding affinity relative to WT with a trend toward an increased sensitivity to 4C*m*C activation and a significant attenuation of Mg^{2+} inhibition relative to WT. However, RyR1 from R163C Het mice had a 2.1-fold decrease in maximal [^{3}H]ryanodine binding capacity. This decrease in binding capacity may be attributed to heterozygosity, which can lead to heterogeneity in the composition of the RyR1 tetramer.

Conclusions

The results presented demonstrate that the newly developed R163C Het mouse line is a valid animal model for studying the largely unknown pathophysiology of MH. Having shown that this mouse is a valid model for human MH will now allow us to study it and other mice with different MH mutations to discover the mechanisms for how diverse mutations in RyR1 produce a similar phenotype. MH is most acutely manifested in skeletal muscle upon exposure to depolarizing neuromuscular blocking agents such as succinylcholine, halogenated alkane general anesthetics such as halothane, and temperature stress.[40] However, most of our knowledge of the molecular, cellular, and pathophysiologic mechanisms conferring MH susceptibility has come from porcine stress syndrome attributed to Hom mutation R615C. Availability of R163C Het and other MH mice will permit detailed investigation of both clinical and subclinical manifestations of this pharmacogenetic disorder, whose etiology likely extends to tissues other than skeletal muscle. RyR1 is expressed in brain as well as skeletal muscle, but to date, it has not been possible to study possible phenotypic changes caused by $_{MH}$ RyR1 expressed in the brain. Evidence of a possible immunologic contribution to clinical MH/CCD has been suggested by Ducreux *et al.*,[34] who found myotubes isolated from MH/CCD patients release significantly higher levels of the proinflammatory cytokine interleukin 6 compared with myotubes cultured from WT or other MH patients. Moreover, B cells express functional RyR1,[41] and B cells isolated from human MH and CCD patients have altered responsiveness to caffeine, 4-C*m*C, and halothane,[41,42] suggesting gene–environment interactions that may directly affect B-cell functions. More recently, dendritic cells were also shown to express functional RyR1 protein in subplasmalemmal puncta and within dendrites.[43] Dendritic cells are antigen-presenting cells whose primary purpose is to acquire antigens derived from self or nonself sources and present them to naive T and B cells.[44] Ca^{2+} signaling plays an important role in the function of dendritic cells, although the pathways responsible have only recently received attention.[43,45] Thus, in addition, its important roles in excitation–contraction coupling, WT, and MH RyR1 proteins are likely to play intrinsic roles in regulating varied aspects of central nervous system and immune system function and dysfunction. The availability of R613C and other MH mice will now permit investigation of MH susceptibility as a multisystem disorder.

The authors thank Matthew Newhouse, Bsc. Grad. Dip., Helen Taylor (Research Technician), and Vane (Wayne) Damcevski, Ass. Dip. App. Science, at The John Curtin School of Medical Research, The Australian National University, Canberra, Australian Capital Territory, Australia, for expert technical help in generating the mice.

References

1. Ahern CP, Milde JH, Gronert GA: Electrical stimulation triggers porcine malignant hyperthermia. Res Vet Sci 1985; 39:257–8
2. Britt BA: Malignant hyperthermia. Clin Anesth 1975; 11:61–74
3. Britt BA, Kalow W: Malignant hyperthermia: A statistical review. Can Anaesth Soc J 1970; 17:293–315
4. Fujii J, Otsu K, Zorzato F, de Leon S, Khanna VK, Weiler JE, O'Brien PJ, MacLennan DH: Identification of a mutation in porcine ryanodine receptor associated with malignant hyperthermia. Science 1991; 253:448–51
5. Roberts MC, Mickelson JR, Patterson EE, Nelson TE, Armstrong PJ, Brunson DB, Hogan K: Autosomal dominant canine malignant hyperthermia is caused by a mutation in the gene encoding the skeletal muscle calcium release channel (RYR1). ANESTHESIOLOGY 2001; 95:716–25
6. Aleman M, Riehl J, Aldridge BM, Lecouteur RA, Stott JL, Pessah IN: Association of a mutation in the ryanodine receptor 1 gene with equine malignant hyperthermia. Muscle Nerve 2004; 30:356–65
7. Nelson TE: Malignant hyperthermia: A pharmacogenetic disease of Ca++ regulating proteins. Curr Mol Med 2002; 2:347–69
8. Monnier N, Procaccio V, Stieglitz P, Lunardi J: Malignant-hyperthermia susceptibility is associated with a mutation of the alpha 1-subunit of the human dihydropyridine-sensitive L-type voltage-dependent calcium-channel receptor in skeletal muscle. Am J Hum Genet 1997; 60:1316–25
9. Louis CF, Balog EM, Fruen BR: Malignant hyperthermia: An inherited disorder of skeletal muscle Ca+ regulation. Biosci Rep 2001; 21:155–68
10. Yang T, Ta TA, Pessah IN, Allen PD: Functional defects in six ryanodine receptor isoform-1 (RyR1) mutations associated with malignant hyperthermia and their impact on skeletal excitation-contraction coupling. J Biol Chem 2003; 278:25722–30
11. Lopez JR, Linares N, Pessah IN, Allen PD: Enhanced response to caffeine and 4-chloro-m-cresol in malignant hyperthermia-susceptible muscle is related in part to chronically elevated resting [Ca2+]i. Am J Physiol Cell Physiol 2005; 288:C606–12
12. Lopez JR, Allen P, Alamo L, Ryan JF, Jones DE, Sreter F: Dantrolene prevents the malignant hyperthermic syndrome by reducing free intracellular calcium concentration in skeletal muscle of susceptible swine. Cell Calcium 1987; 8:385–96
13. Lopez JR, Contreras J, Linares N, Allen PD: Hypersensitivity of malignant hyperthermia–susceptible swine skeletal muscle to caffeine is mediated by high resting myoplasmic [Ca^{2+}]. ANESTHESIOLOGY 2000; 92:1799–806
14. Harrison GG: Control of the malignant hyperpyrexic syndrome in MHS swine by dantrolene sodium. Br J Anaesth 1975; 47:62–5
15. Quane KA, Healy JM, Keating KE, Manning BM, Couch FJ, Palmucci LM, Doriguzzi C, Fagerlund TH, Berg K, Ording H, Bendixen D, Mortier W, Linz U, Muller CR, McCarthy TV: Mutations in the ryanodine receptor gene in central core disease and malignant hyperthermia. Nat Genet 1993; 5:51–5
16. Szabo P, Mann JR: Expression and methylation of imprinted genes during *in vitro* differentiation of mouse parthenogenetic and androgenetic embryonic stem cell lines. Development 1994; 120:1651–60
17. Campbell HD, Fountain S, McLennan IS, Berven LA, Crouch MF, Davy DA, Hooper JA, Waterford K, Chen KS, Lupski JR, Ledermann B, Young IG, Matthaei KI: Fliih, a gelsolin-related cytoskeletal regulator essential for early mammalian embryonic development. Mol Cell Biol 2002; 22:3518–26
18. Lomeli H, Ramos-Mejia V, Gertsenstein M, Lobe CG, Nagy A: Targeted

insertion of Cre recombinase into the TNAP gene: Excision in primordial germ cells. Genesis 2000; 26:116–7

19. Wang Y, Fraefel C, Protasi F, Moore RA, Fessenden JD, Pessah IN, Di-Francesco A, Breakefield X, Allen PD: HSV-1 amplicon vectors are a highly efficient gene delivery system for skeletal muscle myoblasts and myotubes. Am J Physiol Cell Physiol 2000; 278:C619–26

20. Brooks SP, Storey KB: Bound and determined: A computer program for making buffers of defined ion concentrations. Anal Biochem 1992; 201:119–26

21. Chelu MG, Goonasekera SA, Durham WJ, Tang W, Lueck JD, Riehl J, Pessah IN, Zhang P, Bhattacharjee MB, Dirksen RT, Hamilton SL: Heat- and anesthesia-induced malignant hyperthermia in an RyR1 knock-in mouse. FASEB J 2006; 20:329–30

22. Denborough MA, Collins SP, Hopkinson KC: Rhabdomyolysis and malignant hyperpyrexia. BMJ (Clin Res Ed) 1984; 288:1878

23. Bagshaw RJ, Cox RH, Knight DH, Detweiler DK: Malignant hyperthermia in a Greyhound. J Am Vet Med Assoc 1978; 172:61–2

24. Rodrigues SF, de Oliveira MA, Martins JO, Sannomiya P, de Cassia Tostes R, Nigro D, Carvalho MH, Fortes ZB: Differential effects of chloral hydrate- and ketamine/xylazine-induced anesthesia by the s.c. route. Life Sci 2006; 79:1630–7

25. Ward A, Chaffman MO, Sorkin EM: Dantrolene: A review of its pharmacodynamic and pharmacokinetic properties and therapeutic use in malignant hyperthermia, the neuroleptic malignant syndrome and an update of its use in muscle spasticity. Drugs 1986; 32:130–68

26. Gallant EM, Lentz LR: Excitation-contraction coupling in pigs heterozygous for malignant hyperthermia. Am J Physiol 1992; 262:C422–6

27. Tong J, Oyamada H, Demaurex N, Grinstein S, McCarthy TV, MacLennan DH: Caffeine and halothane sensitivity of intracellular Ca2+ release is altered by 15 calcium release channel (ryanodine receptor) mutations associated with malignant hyperthermia and/or central core disease. J Biol Chem 1997; 272: 26332–9

28. Treves S, Larini F, Menegazzi P, Steinberg TH, Koval M, Vilsen B, Andersen JP, Zorzato F: Alteration of intracellular Ca2+ transients in COS-7 cells transfected with the cDNA encoding skeletal-muscle ryanodine receptor carrying a mutation associated with malignant hyperthermia. Biochem J 1994; 301:661–5

29. Lynch PJ, Krivosic-Horber R, Reyford H, Monnier N, Quane K, Adnet P, Haudecoeur G, Krivosic I, McCarthy T, Lunardi J: Identification of heterozygous and homozygous individuals with the novel RYR1 mutation Cys35Arg in a large kindred. Anesthesiology 1997; 86:620–6

30. Rueffert H, Olthoff D, Deutrich C, Thamm B, Froster UG: Homozygous and heterozygous Arg614Cys mutations (1840C–>T) in the ryanodine receptor gene co-segregate with malignant hyperthermia susceptibility in a German family. Br J Anaesth 2001; 87:240–5

31. López JR, Alamo L, Caputo C, Wikinski J, Ledezma D: Intracellular ionized calcium concentration in muscles from humans with malignant hyperthermia. Muscle Nerve 1985; 8:355–8

32. Lopez JR, Lopez M, Allen P: Dantrolene reduces myoplasmic free [Ca2+] in patients with malignant hyperthermia. Acta Cient Venez 1990; 41:135–7

33. Lopez JR, Allen PD, Alamo L, Jones D, Sreter FA: Myoplasmic free [Ca2+] during a malignant hyperthermia episode in swine. Muscle Nerve 1988; 11:82–8

34. Ducreux S, Zorzato F, Muller C, Sewry C, Muntoni F, Quinlivan R, Restagno G, Girard T, Treves S: Effect of ryanodine receptor mutations on interleukin-6 release and intracellular calcium homeostasis in human myotubes from malignant hyperthermia-susceptible individuals and patients affected by central core disease. J Biol Chem 2004; 279:43838–46

35. Wehner M, Rueffert H, Koenig F, Neuhaus J, Olthoff D: Increased sensitivity to 4-chloro-m-cresol and caffeine in primary myotubes from malignant hyperthermia susceptible individuals carrying the ryanodine receptor 1 Thr2206Met (C6617T) mutation. Clin Genet 2002; 62:135–46

36. Weiss RG, O'Connell KM, Flucher BE, Allen PD, Grabner M, Dirksen RT: Functional analysis of the R1086H malignant hyperthermia mutation in the DHPR reveals an unexpected influence of the III-IV loop on skeletal muscle EC coupling. Am J Physiol Cell Physiol 2004; 287:C1094–102

37. Pessah IN, Stambuk RA, Casida JE: Ca2+-activated ryanodine binding: Mechanisms of sensitivity and intensity modulation by Mg2+, caffeine, and adenine nucleotides. Mol Pharmacol 1987; 31:232–8

38. Herrmann-Frank A, Richter M, Lehmann-Horn F: 4-Chloro-m-cresol: A specific tool to distinguish between malignant hyperthermia-susceptible and normal muscle. Biochem Pharmacol 1996; 52:149–55

39. Mickelson JR, Gallant EM, Litterer LA, Johnson KM, Rempel WE, Louis CF: Abnormal sarcoplasmic reticulum ryanodine receptor in malignant hyperthermia. J Biol Chem 1988; 263:9310–5

40. Gronert GA: Dantrolene in malignant hyperthermia (MH)–susceptible patients with exaggerated exercise stress (letter). Anesthesiology 2000; 93:905

41. Sei Y, Gallagher KL, Basile AS: Skeletal muscle type ryanodine receptor is involved in calcium signaling in human B lymphocytes. J Biol Chem 1999; 274:5995–6002

42. Girard T, Cavagna D, Padovan E, Spagnoli G, Urwyler A, Zorzato F, Treves S: B-lymphocytes from malignant hyperthermia-susceptible patients have an increased sensitivity to skeletal muscle ryanodine receptor activators. J Biol Chem 2001; 276:48077–82

43. Goth SR, Chu RA, Pessah IN: Oxygen tension regulates the *in vitro* maturation of GM-CSF expanded murine bone marrow dendritic cells by modulating class II MHC expression. J Immunol Methods 2006; 308:179–91

44. Creusot RJ, Mitchison NA: How DCs control cross-regulation between lymphocytes. Trends Immunol 2004; 25:126–31

45. O'Connell PJ, Klyachko VA, Ahern GP: Identification of functional type 1 ryanodine receptors in mouse dendritic cells. FEBS Lett 2002; 512:67–70